Stochastic Geometry-based Analysis of Multiple Region Reverse Frequency Allocation Scheme in Downlink HetNets

Rehan Zahid and Syed Ali Hassan
School of Electrical Engineering & Computer Science (SEECS)
National University of Sciences & Technology (NUST), Islamabad, Pakistan 44000
Email: {12mseerzahid, ali.hassan}@seecs.edu.pk

***Abstract*—Femtocell access points (FAPs) are low-powered and small-sized base stations that provide high data rates and coverage to the indoor users. Because of their operation in the same spectrum as that of macrocells, interference becomes a major problem. Reverse frequency allocation (RFA) is one of the robust schemes, which mitigate the interference by transfering it from the macrocell base station (MBS) to the macrocell user equipments (MUEs), particularly in the downlink. In this paper, we provide a multiple region 2-tier downlink model using the RFA scheme. We derive a closed-form expression for the coverage probability of femtocell user equipment (FUE) using different RFA schemes under open access mode. Where FAPs and MUEs are modeled as independent Poisson point process (PPP). Using simulations, we show that for reasonable values of signal-to-interference ratio, multiple regions enhance the coverage probability of an FUE. It is shown that a 4-region RFA outperforms the other RFA schemes at different densities of FAPs and MUEs as well as for different values of threshold for the same set of parameters.**

***Index Terms*—Reverse frequency allocation, heterogeneous cellular networks, Poisson point process (PPP), interference, frequency reuse.**

I. Introduction

The rapid increase in the proliferation of wireless devices has increased the requirements of capacity. Wireless networks mainly comprises two technologies, the wireless cellular networks, which provide the voice communication to users having high mobility and wireless local area networks (WLANs) that enable the communication to users with high data rates but with limited mobility. To provide high data rates with good coverage capabilities, femtocells and heterogeneous networks (HetNets) are becoming attractive. Femtocell is a low-powered, and small-sized base station with less complexity that provides high data rates and improves the quality of service to the indoor users. A study shows that about 70% of data traffic and 50% of voice calls are probable to originate from indoor users [1]. The fundamental purpose of the femtocell is to enable the communication with high data rates and good quality of service to indoor users by offloading the data traffic from the main macro base station (MBS), which is an expensive radio resource. The femtocell base station is also known as femtocell access point (FAP), which is installed by the users in their premises. Due to homogeneous deployment of femtocells in macro-cellular network area, interference is one of the main problem due to the same spectrum utilized by the femto-cellular and overlaid macro-cellular network. This interference is generally categorized as co-tier and cross-tier interference. Co-tier interference is usually caused by the network elements that belongs to the same tiers. Whereas, cross-tier interference is caused by the network elements that belongs to the different tiers.

The authors gratefully acknowledge the grant from Higher Education Commission (HEC), Pakistan for sponsoring this research work.

In order to build a communication link among the base station (BS) and its intended user, signal-to-interference plus noise ratio (SINR) must be greater than a pre-defined threshold. To achieve the targeted SINR, these interferences must be minimized. To avoid these interferences, many schemes have been proposed, which allocates the frequency in such a way that the interference can be minimized to a significant level. The deployment of femtocells has significant impact on the selection of these schemes. One of the schemes is *static frequency-reuse scheme* in which the available spectrum is allocated to the femtocell and macrocell separately [2]. In *shared frequency band scheme*, the total available spectrum is shared among the femtocell and overlaid macrocell, while the whole spectrum is allocated to the macrocell and the portion of the whole spectrum is allocated to the femtocell in case of *sub-band frequency reuse scheme*.

In this paper, we used a variant of shared frequency band scheme named as *reverse frequency allocation* (RFA), in which the whole cell is divided into multiple non-overlapping regions and the available spectrum is divided into subbands that are used in each region. By dividing the cell into multiple regions, we reduce the interferers that are using the same frequency carriers. Moreover, the spectral efficiency of the entire network will not be disturbed, because the average number of users in each region will also be reduced. The objective of this paper is to provide an analytical model for heterogeneous networks using *reverse frequency allocation scheme*, and to provide the correct analysis of important metrics like coverage probability and statistics of signal-to-interference ratio.

978-1-4799-5344-8/15/$31.00 ©2015 IEEE

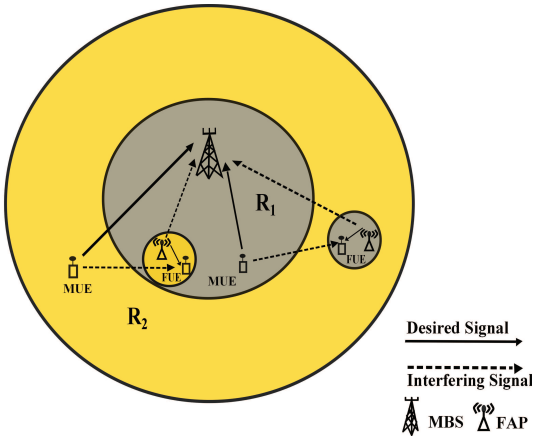

Fig. 1: 2-RFA interfering scenarios; only downlink FUEs scenarios are shown.

A. Related Work

A comprehensive and complete introduction of femtocells with all of its interference scenarios is presented in [3], along with other papers such as [4]-[7]. The authors proposed an 2-region RFA scheme and compare it with others conventional methods of frequency allocation. Using extensive simulations, they showed that the 2-region RFA outperforms the other conventional methods of frequency allocation in term of throughput particularly in the downlink operations [8]. A general K-tier downlink model for HetNets is proposed that gives the simple mathematical expessions for most of the important metrices like SINR statistics, coverage probability and average rates. The major drawback is that the model does not consider frequency reuse, power control or any other form of the interference management techniques [9].

A well accepted and most popular model is the conventional two dimensional hexagonal grid model. This model is extensively used for system level simulations [10][11]. Another model that allows the random deployment of base stations in form of Poisson point process (PPP) [12]-[14]. Such models are more accurate and suitable for random deployment of femtocells. Moreover, the difference between random and actual deployment of base stations is small, even for macro base stations (MBSs) deployment. Recent research [15] showed that the deployment of macrocell base stations (MBSs) drawn from PPP is accurate as two dimensional hexagonal grid model, when compared to actual 4G network. The model also enables us to use the important mathematical tools from stochastic geometry to perform the analysis of HetNets more accurately [16][17].

The fundamental contribution of this paper is to provide a multiple region 2-tier downlink model using the RFA scheme. In the next section, we provide a network model operating on the RFA mechanism. The analytical model consists of two independent tiers of FAPs and MUEs that are modeled as independent PPPs. We derive a closed-form expression of average coverage probability for FUE using various forms of 4-RFA algorithm under open access mode. The simulation results are presented in Section IV while the paper concludes in Section V.

II. System Model

Consider an RFA scheme for a single cell, in which the whole cell is divided into K non-overlapping regions. Likewise, the available frequency spectrum, F, is divided into K frequency subbands, such that $F = \bigcup_{i=1}^{K} F_i$. The K frequency subbands are further divided into uplink and downlink frequency carriers for every ith region, such that $F = [F_{iA} + F_{iB}]$; where $i = \{1, 2, ...K\}$. In case of 2-RFA, the two disjoint regions R_1 and R_2 are assigned subbands F_1 and F_2, respectively. The uplink band of R_1-MUEs is reused by the downlink FUEs in R_2. Similarly, the uplink band of R_2-MUEs is reused by the downlink FUEs in R_1. Using such frequency allocation, the FUEs receive interference from a subset of uplink MUEs that are using the same frequency carriers, instead of MBS, which is a great source of interference. Similar procedure is followed in the other subbands, i.e., the downlink MUEs in R_1 utilize the same band as FUEs for uplink in R_2 and the downlink MUEs in R_2 use the same band as uplink FUEs in R_1. In this case the downlink MUEs in R_1 and R_2 only face the cross-tier interference from a subset of uplink FUEs in R_2 and R_1, respectively.

We consider a worst case scenario for FUEs in both regions, in which all the uplink MUEs in R_2 and neighboring downlink FAPs in R_1 produce the cross-tier and co-tier interference to the R_1-FUEs, repectively. The same is the case with R_2-FUEs, i.e., all the uplink R_1-MUEs and neighboring downlink FAPs in R_2 generate the cross-tier and co-tier interference, respectively. Since all the FAPs in R_1 and R_2 are operating on the same frequency carriers F_{2A} and F_{1A} for downlink, respectively, so co-tier interference will also occur. Hence the FUEs in each region receive two types of interferences, one is the co-tier interference from neighboring FAPs in the same region, and other is the cross-tier interference from MUEs in the other region. Similarly, in the case of 4-RFA, an entire cell is divided into four disjoint regions. i.e., R_1, R_2, R_3 and R_4 and likewise the spectrum. The four subbands are further divided into uplink and downlink frequency carriers. i.e., $F = [F_{iA} + F_{iB}]$; where $i = \{1, 2, ...4\}$. Now F_{1A} and F_{1B} are used by MUEs for uplink and downlink in R_1, F_{2A} and F_{2B} are used by the MUEs in R_2 for uplink and downlink, respectively. The same is the case for MUEs in R_3 and R_4. Since F_{1A} and F_{1B} are used by the R_1-MUEs for uplink and downlink operations, so it is desired to reuse these frequency carriers to one of the downlinks and uplinks of FUEs in a distant region R_3, respectively. Similarly, F_{2A} and F_{2B} which are used by the MUEs in R_2 for uplink and downlink are also utilized by the R_4-FUEs for downlink and uplink operations, respectively. In case of R_1-MUEs, they receive interference from uplink FUEs in R_3 while R_2-MUEs receive interference from uplink FUEs in R_4. Hence we make two interfering regions; R_1 & R_3 and R_2 & R_4. The interference will be minimum if the interfering regions are as far as possible.

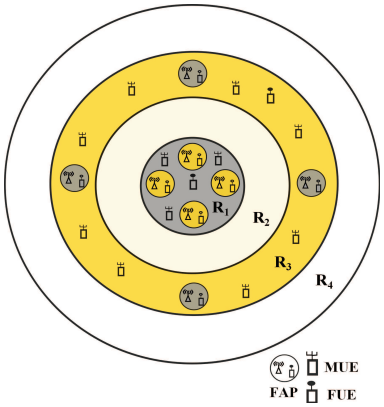

Fig. 2: 4-RFA geometry of 2-tier Hetnet; only first scenario is shown.

TABLE I: 4-RFA interference scenarios

Scenarios	FUE location	Interference
First	FUE in R_1	uplink MUEs in R_3 & downlink FAPs in R_1
Second	FUE in R_2	uplink MUEs in R_4 & downlink FAPs in R_2
Third	FUE in R_3	uplink MUEs in R_1 & downlink FAPs in R_3
Fourth	FUE in R_4	uplink MUEs in R_2 & downlink FAPs in R_4

In summary, R_1-FUEs and R_2-FUEs receive interference from the uplink MUEs in R_3 and R_4, respectively. The R_3-FUEs and R_4-FUEs receives interference from the uplink MUEs in R_1 and R_2, respectively. The R_1-MUEs and R_2-MUEs receive interference from the uplink FUEs in R_3 and R_4, respectively, while R_3 and R_4-MUEs receive interference from uplink FUEs in R_1 and R_2, respectively.

III. Stochastic Modelling of the Network

Consider a 4-RFA downlink geometry of a 2-tier HetNet for a single cell. The first tier is the macrocellular network while the femtocells form the second tier of the network. Each tier may differ on the values of transmit power, thresholds and user densities per unit area. In this study, we are intrested in calculating the average success probability of an FUE when the FUE is placed in any region of the 4-RFA network and receives co-tier and cross-tier interferences as discussed in the previous section. Since there are four regions in 4-RFA, four FUE location scenarios arise, which are shown in Table I. In the following, we discuss the first scenario by assuming the worst case in which R_1-FUE receives interference from all the neighboring downlink FAPs in the same region R_1 and from all the uplink MUEs in R_3. We locate the FUE anywhere in R_1, which connects to one FAP in R_1 only if its downlink received signal-to-interference plus noise ratio from that FAP is greater than a pre-defined threshold τ. Since the FUE, when connected to a FAP, gets interference from neighboring FAPs in R_1 and MUEs in R_3; we model the distribution of FAPs and MUEs as spatial PPPs, $\phi_j^{(i)}$, each having a density of $\lambda_j^{(i)}$, where j denotes the tier of the network, $j \in \{1,2\}$, and i denotes the ith region of a cell, where $i = 2^M$ and $M = \mathbb{Z}^+$. Hence for 4-RFA, $M = 2$ and $i = 4$. Thus for each of the four regions R_1, R_2, R_3 and R_4, we have two independent PPPs; one for uplink MUEs with density $\lambda_1^{(i)}$, and one for FAPs with density $\lambda_2^{(i)}$. We first divide the entire cell into four regions and then distribute the FAPs and MUEs as independent PPPs in each region. All the FAPs and MUEs have equal density in each region. For example, for 1000 FAPs and MUEs, each region consists of 250 FAPs and MUEs, respectively. Moreover, we let r_1 be the radius of region R_1. Similarly r_i denotes the annulus region between $R_i - R_{i-1}$, $i \in \{2,3,4\}$.

Let $y_j^{(i)}$ denotes the set of all locations of FAPs or MUEs in the ith region. The downlink transmission of FAP undergoes Rayleigh fading and path loss. The squared envelope of the channel fading between two terminals is represented by $h_{y_j}^{(i)}$, which consists of independently and identically distributed (i.i.d) random variables (RVs) that are drawn from an exponentional distribution. The path loss function is given by $\ell(y_j^{(i)}) = \| y_j^{(i)} \|^{-\alpha}$, where α is the path loss exponent. Therefore, the received signal-to-interference ratio for R_1-FUE is given as

$$\gamma = \frac{P_2 h_{y_2}^{(1)} \| y_2^{(1)} \|^{-\alpha}}{\sum_{y \in \phi_2^{(1)} \setminus y_2^{(1)}} P_2 h_y^{(1)} \| y \|^{-\alpha} + \sum_{y \in \phi_1^{(3)}} P_1 h_y^{(3)} \| y \|^{-\alpha}}. \tag{1}$$

where P_j is the transmit power of MUEs or FAPs for $j = 1$ and $j = 2$, respectively. The reason for considering SIR is that the self interference dominates the noise in cellular networks even with modest density, hence we ignore the effects of thermal noise in the sequel. We now present the coverage probability of an FUE as the following theorem.

Theorem 1. *The coverage probability of R_1-FUE in a 4-RFA scenario under SIR connectivity is given by*

$$P_c \leq \frac{\lambda_2^{(1)} \pi}{A} \left[1 - \exp(-A r_1^2)\right]$$

where $A = \left(\frac{\tau}{P_2}\right)^{2/\alpha} \left(C_1^{(3)} \lambda_1^{(3)} (P_1)^{2/\alpha} + C_2^{(1)} \lambda_2^{(1)} (P_2)^{2/\alpha}\right)$

$$C_1^{(3)} = 2\pi \int_{r_2}^{r_3} \frac{r}{1 + r^\alpha} \mathrm{d}r, \text{ and } C_2^{(1)} = 2\pi \int_0^{r_1} \frac{r}{1 + r^\alpha} \mathrm{d}r.$$

Proof. The coverage probability is given as

$$\begin{aligned} P_c &= \mathbb{P}\left(\bigcup_{y_2^{(1)} \in \phi_2^{(1)}} \gamma(y_2^{(1)}) > \tau \right) \\ &= \mathbb{E}\left[\mathbf{1}\left(\bigcup_{y_2^{(1)} \in \phi_2^{(1)}} \gamma(y_2^{(1)}) > \tau \right) \right] \\ &\leq \mathbb{E} \sum_{y_2^{(1)} \in \phi_2^{(1)}} \left(\gamma(y_2^{(1)}) > \tau \right) \qquad (2) \\ &= \lambda_2^{(1)} \int_{R^2} \mathbb{P}\left(\frac{P_2 h_{y_2}^{(1)} \ell(y_2^{(1)})}{I_y} > \tau \right) \mathrm{d}y_2^{(1)} \qquad (3) \\ &= \lambda_2^{(1)} \int_{R^2} \mathcal{L}_{I_y}\left(\frac{\tau}{P_2 \ell(y_2^{(1)})} \right) \mathrm{d}y_2^{(1)}, \qquad (4) \end{aligned}$$

where (2) shows that the equality holds only for SIR threshold $\tau \geq 1$, otherwise the right hand side becomes the upper bound of the coverage probability and (3) follows from the Campbell Mecke Theorem [16] and (4) follows from the assumption that the channel gains are assumed to be Rayleigh distributed. Here I_y is the cumulative interference that includes both co-tier and cross-tier inteference and $\mathcal{L}_{I_y}(.)$ is the Laplace transform of the cumulative interference from all the interferers of both tiers, when an FUE is connected to its desired FAP. Since the PPPs are stationary, hence the interference is not dependent upon the location y. Therefore, $\mathcal{L}_{I_y}(.)$ is represented by $\mathcal{L}_I(.)$, which is further given as

$$\mathcal{L}_I(s) = \mathbb{E}\left[\prod_{y\in\phi_1^{(3)}} \exp(-sP_1 h_y^{(3)}\ell(y))\right] \times \mathbb{E}\left[\prod_{y\in\phi_2^{(1)}\setminus y_2^{(1)}} \exp(-sP_2 h_y^{(1)}\ell(y))\right], \quad (5)$$

As the fading random variables are independent, so (5) becomes

$$\mathcal{L}_I(s) = \mathbb{E}_{\phi_1^{(3)}}\left[\prod_{y\in\phi_1^{(3)}} \mathbb{E}_h[\exp(-sP_1 h_y^{(3)}\ell(y))]\right] \times \mathbb{E}_{\phi_2^{(1)}}\left[\prod_{y\in\phi_2^{(1)}\setminus y_2^{(1)}} \mathbb{E}_h[\exp(-sP_2 h_y^{(1)}\ell(y))]\right], \quad (6)$$

$$\mathcal{L}_I(s) = \mathbb{E}_{\phi_1^{(3)}}\left[\prod_{y\in\phi_1^{(3)}} \frac{1}{1+sP_1\ell(y)}\right] \times \mathbb{E}_{\phi_2^{(1)}}\left[\prod_{y\in\phi_2^{(1)}\setminus y_2^{(1)}} \frac{1}{1+sP_2\ell(y)}\right], \quad (7)$$

where (7) follows from the assumption that the channel gains are Rayleigh faded. We now have

$$\mathcal{L}_I(s) = \exp\left(-\lambda_1^{(3)}\int_{r_2}^{r_3}\left(1-\frac{1}{1+sP_1 \parallel y_1^{(3)} \parallel^{-\alpha}}\right)\mathrm{d}y_1^{(3)}\right) \times \exp\left(-\lambda_2^{(1)}\int_{0}^{r_1}\left(1-\frac{1}{1+sP_2 \parallel y_2^{(1)} \parallel^{-\alpha}}\right)\mathrm{d}y_2^{(1)}\right), \quad (8)$$

where (8) follows from the probability generating functional (PGFL) of underlying PPPs [16]. Eq. (8) can be rewritten as

$$\mathcal{L}_I(s) = \exp\left(-2\pi\lambda_1^{(3)}(sP_1)^{2/\alpha}\int_{r_2}^{r_3}\frac{r}{1+r^\alpha}\mathrm{d}r\right) \times \exp\left(-2\pi\lambda_2^{(1)}(sP_2)^{2/\alpha}\int_{0}^{r_1}\frac{r}{1+r^\alpha}\mathrm{d}r\right), \quad (9)$$

where (9) results from converting the cartesian coordinates to polar coordinates. It can be further simplified as

$$\mathcal{L}_I(s) = \exp\left[-(s)^{2/\alpha}C_1^{(3)}\lambda_1^{(3)}(P_1)^{2/\alpha}\right] \times \exp\left[-(s)^{2/\alpha}C_2^{(1)}\lambda_2^{(1)}(P_2)^{2/\alpha}\right], \quad (10)$$

where

$$C_1^{(3)} = 2\pi\int_{r_2}^{r_3}\frac{r}{1+r^\alpha}\mathrm{d}r,$$

and

$$C_2^{(1)} = 2\pi\int_{0}^{r_1}\frac{r}{1+r^\alpha}\mathrm{d}r.$$

For a special case of $\alpha = 2$,

$$C_1^{(3)} = \pi\log\left[\frac{1+r_3^2}{1+r_2^2}\right],\ and\ \ C_2^{(1)} = \pi\log\left[1+r_1^2\right].$$

For other values of α, $C_j^{(i)}$'s can be computed numerically. By using (4) and (10), the coverage probability of R_1-FUE is given by

$$P_c^{(1)} \leq \lambda_2^{(1)}\times \int_0^{r_1} e^{\left(-\left(\frac{\tau}{P_2}\right)^{2/\alpha}\left(C_1^{(3)}\lambda_1^{(3)}(P_1)^{2/\alpha}+C_2^{(1)}\lambda_2^{(1)}(P_2)^{2/\alpha}\right)\|y_2^{(1)}\|^2\right)}\mathrm{d}y_2^{(1)}. \quad (11)$$

By solving the integeral, (11) can be further simplified to

$$P_c \leq \frac{\lambda_2^{(1)}\pi}{A}\left[1-\exp(-Ar_1^2)\right]. \quad (12)$$

■

In the second scenario, R_2-FUE receives the interference from all the neighboring downlink FAPs in the same region R_2 and from all the uplink MUEs in R_4. Hence using the same procedure as previously described, the coverage probability of the R_2-FUE is given by

$$P_c^{(2)} \leq \lambda_2^{(2)}\times \int_{r_1}^{r_2} e^{\left(-\left(\frac{\tau}{P_2}\right)^{2/\alpha}\left(C_1^{(4)}\lambda_1^{(4)}(P_1)^{2/\alpha}+C_2^{(2)}\lambda_2^{(2)}(P_2)^{2/\alpha}\right)\|y_2^{(2)}\|^2\right)}\mathrm{d}y_2^{(2)}. \quad (13)$$

where

$$C_1^{(4)} = 2\pi\int_{r_3}^{r_4}\frac{r}{1+r^\alpha}\mathrm{d}r,\ and\ \ C_2^{(2)} = 2\pi\int_{r_1}^{r_2}\frac{r}{1+r^\alpha}\mathrm{d}r.$$

Similarly, in case of third and fourth scenario the coverage probability of FUE is given by

$$P_c^{(3)} \leq \lambda_2^{(3)}\times \int_{r_2}^{r_3} e^{\left(-\left(\frac{\tau}{P_2}\right)^{2/\alpha}\left(C_1^{(1)}\lambda_1^{(1)}(P_1)^{2/\alpha}+C_2^{(3)}\lambda_2^{(3)}(P_2)^{2/\alpha}\right)\|y_2^{(3)}\|^2\right)}\mathrm{d}y_2^{(3)}. \quad (14)$$

where

$$C_1^{(1)} = 2\pi\int_{0}^{r_1}\frac{r}{1+r^\alpha}\mathrm{d}r,\ and\ \ C_2^{(3)} = 2\pi\int_{r_2}^{r_3}\frac{r}{1+r^\alpha}\mathrm{d}r.$$

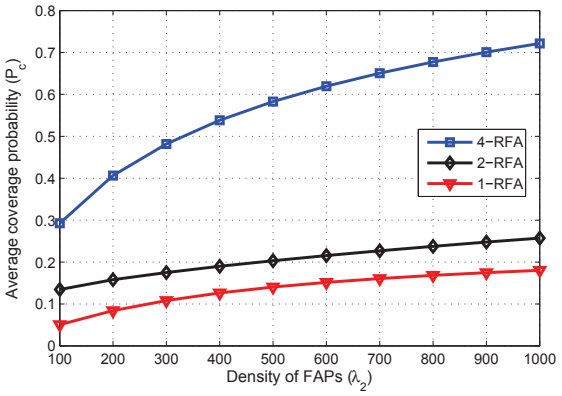

Fig. 3: Average coverage probability of FUE at different density of FAPs (λ_2); $(\lambda_1 = 200,\, \tau = -6.98dB)$

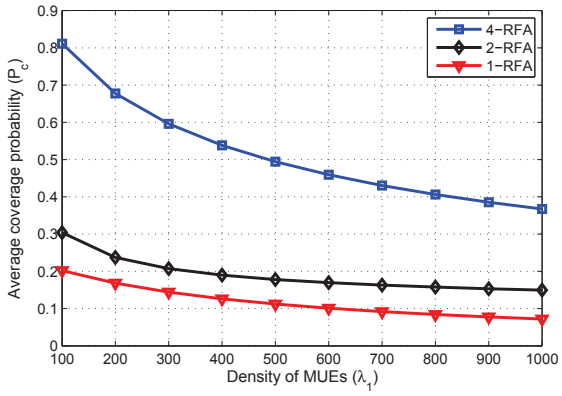

Fig. 4: Average coverage probability of FUE at different density of MUEs (λ_1); $(\lambda_2 = 1600, \tau = -6.98dB)$

$$P_c^{(4)} \leq \lambda_2^{(4)} \times \int_{r_3}^{r_4} e^{\left(-\left(\frac{\tau}{P_2}\right)^{2/\alpha}\left(C_1^{(2)}\lambda_1^{(2)}(P_1)^{2/\alpha}+C_2^{(4)}\lambda_2^{(4)}(P_2)^{2/\alpha}\right)\|y_2^{(4)}\|^2\right)} \mathrm{d}y_2^{(4)}. \tag{15}$$

where

$$C_1^{(2)} = 2\pi \int_{r_1}^{r_2} \frac{r}{1+r^\alpha}\mathrm{d}r, \; and \; C_2^{(4)} = 2\pi \int_{r_3}^{r_4} \frac{r}{1+r^\alpha}\mathrm{d}r.$$

IV. Numerical Results and Performance Analysis

In this section, we present our analytical results for 4-RFA and compare it with other reuse schemes. The transmission power of MUEs and FAPs is fixed to be unity. We conduct the analysis of coverage probability by locating the FUE in any region of the 4-RFA network. Moreover, we consider a worst-case scenario in which all the FAPs are operating at downlink while all the MUEs are operating at uplink in every ith region. The average coverage probability of FUE at different densities of FAPs and MUEs is analyzed for different RFA schemes. In 1-RFA scheme, there is a single cell area and the FUE connects to a FAP having SIR $> \tau$, whereas it receives interference from all other FAPs and MUEs in the same area.

Figs. 3 and 4 shows the average coverage probability of an FUE by varying the densities of FAPs (λ_2) and MUEs (λ_1), in case of different RFA schemes. These graphs analyze the average coverage probability of FUE in a macrocell having a radius of 2 km. The path loss exponent α is taken to be 2. The channel gains $h_{y_j}^{(i)}$ are assumed to be Rayleigh faded.

In Fig. 3, it can be observed that at fixed density of MUEs and threshold value, as the density of FAPs increases, the average coverage probability of the FUE also increases. This increment is due to the fact that as the density of FAPs increases in a fixed region, the probability of FAP to get closer to the FUE also increases, which in turn provide the higher SIR to the FUE. Moreover, it can also be observed that for 1000 FAPs, the average coverage probability is approximately 72%. This upper bound is due to the tighter selection of threshold. For

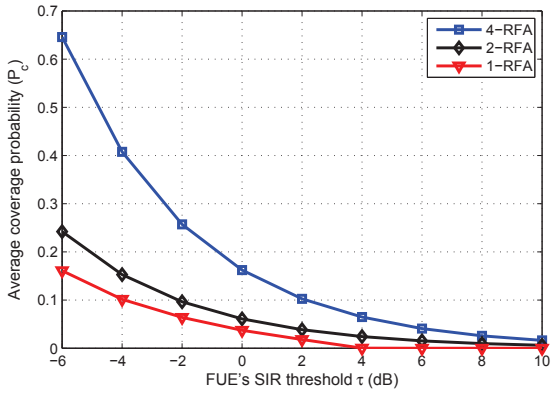

Fig. 5: Average coverage probability of FUE at different SIR threshold (τ); $(\lambda_1 = 200, \lambda_2 = 1600)$

lower values of threshold, i.e., $-10dB$, the average coverage probability nearly approaches to 1. It can also be seen that 4-RFA provides the highest coverage probability for FUE as compared to the other RFA schemes. This is because in case of 4-RFA, the cross-tier interference from uplink MUEs in the distant region is very small due to the large path loss between them as compared to the other RFA schemes, i.e., R_1-FUE receives cross-tier interference from the uplink MUEs in the distant region R_3. Moreover, in 4-RFA, the regions become smaller as compared to the 1 and 2-RFA, which increases the probability of FAPs to get closer to FUE and reduce the number of interferers in each region.

In Fig. 4, it can be seen that at fixed density of FAPs and threshold value, as the density of MUEs increases, the average coverage probability of the FUE decreases. This decrement is due to the fact that the density of uplink MUEs (interferers) increases in each region which in turn increases the cross-tier interference. In case of 4-RFA, the decrement in average coverage probability is much lower as compared to the other RFA schemes. The reason is that the 4-RFA divides the entire

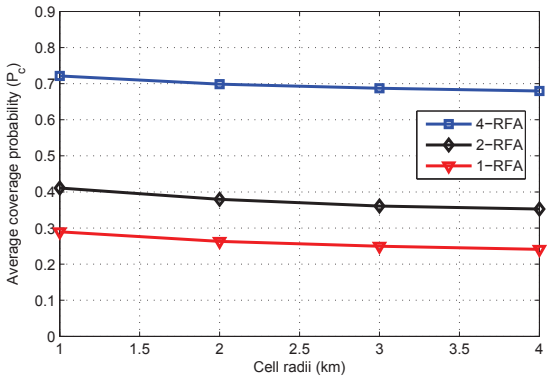

Fig. 6: Average coverage probability of FUE at different cell radius; $(\lambda_1 = 200, \lambda_2 = 1600, \tau = -6.98dB)$

cell in such a way that the each region has less number of interferers as compared to 1 and 2-RFA. For example, if the density of MUEs is 100 in the entire cell, each region of 2-RFA consists of 50 uplink MUEs while each region of 4-RFA consists of 25 uplink MUEs on the average. In 1-RFA, all MUEs are deployed in a single region. Therefore, 4-RFA outperforms the other RFA schemes by assigning less number of interferers in each region.

Fig. 5 shows the coverage probability of an FUE for different values of threshold at fixed densities of MUEs and FAPs. It can be noticed that for lower values of threshold, 4-RFA outperforms the other RFA schemes. The reason is that 4-RFA provides the higher coverage to an FUE because of the reason mentioned earlier. Moreover, in 4-RFA, the regions become smaller as compared to 1 and 2-RFA, which increases the probability of FAPs of getting closer to the FUE. As a result the SIR of FUE in each region becomes greater than the pre-defined threshold.

Fig. 6 shows the coverage probability of an FUE at different cell radius for different RFA schemes. The densities of MUEs(λ_1), FAPs(λ_2) and threshold (τ) value is kept constant. It can be seen that as the radius of the macrocell increases, the coverage probability of FUE almost remains constant for different RFA schemes. This is because when the macrocell radius increases, the path loss between an FUE and the interferers increases. At the same time, the path loss between that FUE and the desired FAP also increases. Therefore, the average coverage probability of the FUE remains same over all the macrocell radii. It can also be observed that the 4-RFA outperforms the other RFA schemes for all macrocell radii due to the aformentioned reasons.

V. CONCLUSION

Dense deployment of FAPs provides high data rates and coverage to the indoor users by offloading the traffic from the macrocell base station (MBS). Reverse frequency allocation is one of the robust schemes, which provides the interference mitigation by transfering the downlink interference from the macrocell base station to the macrocell user equipments. We have provided a multiple region 2-tier downlink model using reverse frequency allocation scheme. The analytical model consists of two independent tiers of MUEs and FAPs that are modeled as independent PPPs. We have derived a closed-form expression of the coverage probability of an FUE using various forms of RFA algorithm under open access mode. The simulation results shows that 4-RFA outperforms the other RFA schemes at different densities of FAPs and MUEs as well as for different values of threshold without distrubing the spectral efficiency of the network. The overall analysis of the RFA for a general user, whether FUE or MUE, with higher multiple regions and multiple cell scenarios is left as a future work. Also in this work, the macrocell region is divided into equal circular areas, however, an optimization problem can be formulated where the region's radii are found optimally to provide better performance.

REFERENCES

[1] Presentations by ABI Research, Picochip, Airvana, IP access, Gartner, Telefonica Espana, "Home access points and femtocells", *2nd Intl. Conf.*. Available: http://www.avrenevents.com/dallasfemto2007/purchase presentations. html

[2] M. Z. Chowdhury, Y. M. Jang, Z. J. Haas, "Cost-effective frequency planning for capacity enhancement of femtocellular networks", *Wireless Personal Commun.*, vol. 60, issue 1, pp. 83-104, Sept. 2011.

[3] T. Zahir, K. Arshad, A. Nakata, K. Moessner, "Interference management in femtocells", *Commun. Surveys Tutorials, IEEE*, vol. 15, no. 1, pp. 293-311, First Quarter 2013.

[4] V. Chandrasekhar, J. G. Andrews and A. Gatherer, "Femtocell networks: a survey", *IEEE Commun. Mag.*, vol. 46, no. 9, pp. 59-67, Sept. 2008.

[5] S.P. Yeh, S. Talwar, S.-C. Lee, and H. Kim, "WiMAX femtocells: A perspective on network architecture, capacity, and coverage", *IEEE Commun. Mag.,* vol. 46, no. 10, pp. 58-65, Oct. 2008.

[6] D. Lpez-Prez, A. Valcarce, G. de la Roche, and J. Zhang, "OFDMA femtocells: A roadmap on interference avoidance", *IEEE Commun. Mag.,* vol. 47, no. 9, pp. 41-48, Sept. 2009.

[7] J. Zhang, de la Roche, E. Liu, "Introduction in Femtocells: Technologies and Deployment", John Wiley Sons, Ltd, Chichester, UK, 2009.

[8] P. Jacob, A. James, A.S. Madhukumar, "Downlink capacity improvement and interference reduction through Reverse Frequency Allocation", *IEEE Intl. Conf. on Commun. Systems,* pp.329-333, 21-23 Nov. 2012.

[9] H. S. Dhillon, R. K. Ganti, F. Baccelli and J. G. Andrews, "Modeling and Analysis of K-Tier Downlink Heterogeneous Cellular Networks", *IEEE Journal on Sel. Areas in Commun.,* vol. 30, no. 3, pp. 550-560, Apr. 2012.

[10] S. Catreux, P. F. Driessen, and L. J. Greenstein, "Simulation results for an interference-limited multiple-input multiple-output cellular system", *IEEE Commun. Lett.,* vol. 4, no. 11, pp. 334-336, Nov. 2000.

[11] A. Ganz, C. M. Krishna, D. Tang, and Z. J. Haas, "On optimal design of multitier wireless cellular systems", *IEEE Commun. Mag.,* vol. 35, no. 2, pp. 88-93, Feb. 1997.

[12] T. X. Brown, "Cellular performance bounds via shotgun cellular systems", *IEEE J. Sel. Areas Commun.,* vol. 18, no. 11, pp. 2443 - 2455, Nov. 2000.

[13] F. Baccelli, M. Klein, M. Lebourges, and S. Zuyev, "Stochastic geometry and architecture of communication networks", *J. Telecomm. Systems,* 1997.

[14] F. Baccelli and S. Zuyev, "Stochastic geometry models of mobile communication networks", *in Frontiers in Queueing. Boca Raton, FL: CRC Press,* 1997, pp. 227-243.

[15] J. G. Andrews, F. Baccelli, and R. K. Ganti, "A tractable approach to coverage and rate in cellular networks", *IEEE Trans. Commun.,* vol. 59, no. 11, pp. 3122 - 3134, Nov. 2011.

[16] D. Stoyan, W. Kendall, and J. Mecke, "Stochastic Geometry and Its Applications", 2nd ed. John Wiley and Sons, 1996.

[17] F. Baccelli and B. Blaszczyszyn, "Stochastic Geometry and Wireless Networks", Now: Foundations and Trends in Networking, 2010.